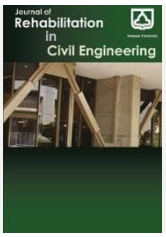

Journal of Rehabilitation in Civil Engineering

Journal homepage: https://civiljournal.semnan.ac.ir/

Effect of Wind Loading Pattern on Shear Lag Phenomenon in Framed-Tube Building

Ashish Singh [1,*]; Piyush Gaikwad [2]; Sasankasekhar Mandal [3]

1. Research Scholar, Department of Civil Engineering, IIT (BHU), Varanasi, India
2. M. Tech. Student, Department of Civil Engineering, IIT (BHU), Varanasi, India
3. Professor, Department of Civil Engineering, IIT (BHU), Varanasi, India

* Corresponding author: *ashishsingh.rs.civ18@iitbhu.ac.in*

ARTICLE INFO

Article history:
Received: 13 October 2022
Revised: 06 June 2023
Accepted: 05 July 2023

Keywords:
Codal provisions;
Framed tube;
Shear lag phenomenon;
Torsional wind load;
Wind loading.

ABSTRACT

High-rise tubular buildings experience the shear lag phenomenon due to wind load. This phenomenon results in tension in upper storey columns that may adversely affect building stability. Shear lag varies with many factors such as building layout, outer peripheral columns spacing, and load applied to the building. Therefore, it is essential to accurately analyze the shear lag phenomenon by considering these factors, especially, with due emphasize on the pattern of the applied wind loading. This paper attempts to study the effect of wind loading pattern on the shear lag phenomenon. Six load cases are taken from American and Canadian codes to analyze the wind load effects on a 40-storeyed tubular building. The results indicate that axial force distribution changes significantly with change in the loading patterns of the building. A difference in axial force distribution is observed between torsional and non-torsional load cases. Axial force in columns in the case of uniform loading is more significant as compared to partial loading cases. Due to loading on half of the face, axial force distribution becomes unsymmetrical, and a minimum axial force in corner columns is observed. Also, notable differences can be seen in the axial force distribution of load cases having both direction loadings compared to single direction loadings. Axial force distributions in cases of both face loading are unsymmetrical for the central column.

E-ISSN: 2345-4423

How to cite this article:
Singh, A., Gaikwad, P., & Mandal, S. (2024). Effect of Wind Loading Pattern on Shear Lag Phenomenon in Framed-Tube Building. Journal of Rehabilitation in Civil Engineering, 12(1), 1-17. https://doi.org/10.22075/jrce.2023.28689.1729

1. Introduction

Tall buildings, constructed in response to urbanization and population growth, face the challenge of addressing increased wind loads as they reach greater heights. Recent advancements in structural systems, dampers, and lighter materials offer potential solutions to mitigate vibrations. Wind loads play a crucial role in tall building design, causing along-wind, across-wind, and torsional vibrations (Fig.1). Along-wind vibrations result from flow turbulence, while vortex shedding and wake excitation typically cause across-wind and torsional vibrations. The trend of irregular-shaped buildings intensifies unbalanced wind loads and torsional moments. Unfortunately, limited studies have evaluated the effects of wind-induced torsional loads on a building's structural elements. Considering wind effects in tall building design is vital, necessitating further investigation into wind-induced torsional forces.

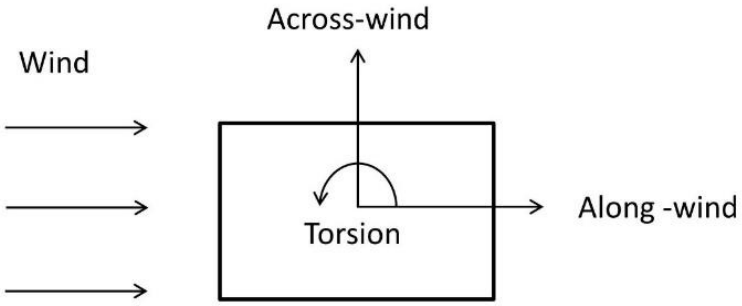

Fig. 1. Direction of wind loading and its component.

To resist the building from the effects of wind load, various types of structural systems may be adopted according to their requirements such as rigid frame systems, braced frames, shear-walled frame systems, outrigger systems, framed-tube systems, braced-tube systems, bundled-tube systems. The framed tube system is one of the most reliable structural systems for resistance against lateral loadings. It consists of closely spaced columns at the periphery of the building and it is connected by deep spandrel beams. Its shape is like a hollow concrete tube. A lateral loading of a box structure will produce the shear lag effect [1–4]. The shear lag phenomenon is therefore more likely to be prominent in tubular structures. The elementary beam theory is violated because it changes the presumptions made about the plane section in box structures and results in non-uniform stress along the sides (Fig. 2). There is greater flexural normal stress at the edge of the flange than in the center (Positive shear lag: Axial force in corner columns exceeds central column, causing higher flexural stress at flange edge than center). Unlike positive shear lag, Foutch and Chang [5] discovered the opposite shear lag anomaly called negative shear lag. (Negative shear lag: Axial force in central column exceeds corner columns, resulting in lower flexural stress at flange edge compared to center). The negative shear lag was also investigated for a composite beam [6]. Singh and Nagpal [7] state that the positive shear lag is found to be the source of negative shear lag. Rovnak and Rovnakova [8] presented a divergent perspective, highlighting the independent nature of positive and negative shear lags. Their observations suggest that these two aspects operate separately from each other. Tube-type structures become less efficient due to the occurrence of shear lag. [9,10]. A precise method for calculating stress and displacement in border columns was proposed by Haji-Kazemi [11] using a cantilever box girder model representative of

the framed tube buildings. Considering shear lag, the performance of the framed tube by assessing the axial stress distribution on the peripheral panels was evaluated by Mahjoub *et al.* [12]. With a given factor, Leonard [13] examined the shear lag effect in the diagrid system. This factor is calculated as the ratio of the axial stress in the corner column to the axial stress in the center of the panel. There have been several studies conducted since then to evaluate the shear lag effect with this factor [14–17]. Shi and Zhang [18] have brought out an updated, more straightforward estimate of the shear lag effect for diagrid systems. Mashhadiali *et al.* [19] compared the shear lag effect between framed tube, diagrid, and hexagrid structural systems with various heights of buildings. They concluded that using truss systems such as hexagrid and diagrid significantly reduced shear lag compared to frame tube system flexible spandrels. Hafner *et al.* [20] conducted a parametric analysis of the shear lag effect in tube structural systems of tall buildings for the purpose of giving recommendations for an optimal design. The relationship between shear lag and the type of lateral loadings (wind & earthquake) on concrete tubular structures has been investigated [21]. An investigation is conducted on the effect of core on shear lag in tubular structures [22]. The significance of shear-lag on axial stress distribution by cracking load is illustrated by [23,24].

Kumari *et al.* [25] investigate the effect of terrain category, aspect ratio, and the number of storeys on the shear lag phenomenon in reinforced cement concrete (RCC) framed tube structures. Torsional motion due to wind can increase the acceleration and displacement near the corner of the building's cross-section, which causes warping of exterior walls and claddings [26]. Even though torsional loads do not pose a threat to the building's safety, they can have a significant impact on the building's serviceability. Torsional vibrations can cause discomfort to the inhabitants because the occupants are more sensitive to torsional acceleration than translational motion [27]. Therefore, torsional loads must be considered appropriately in the design of the tall building. However, there are limited analytical methods available for estimating torsional wind forces and their response. Wind-induced torsional load and response can be obtained from wind tunnel studies. There are finite formulations available in some codes and standards for calculations of the torsional load, such as in ASCE 7-22 [28], NBCC-2020 [29], and Eurocode-2005 [30]. Thus, it is crucial to gain a better understanding of wind-induced torsional loads on tall buildings.

The purpose of this paper is to analyze the variation in shear lag caused by different wind-induced load cases based on ASCE 7-22 and NBCC-2020 code in a 40-storey tubular building to determine the axial force on the external columns so that the peripheral columns can be designed suitably under wind loading. Results from six load cases adopted from American and Canadian codes are compared critically to understand their relative importance. None of the existing studies on shear lag has focused on the multi-directional wind loading along with torsional moments. It is worth noting that the results from this study help in understanding the effect of various wind loading patterns on tubular structures that exhibit shear lag.

2. Codal provisions

A limited amount of information is provided in codes and standards regarding the estimation of wind-induced torsional loads. ASCE 7-22, NBCC 2020, and EN 1991-1-4 (2005) are the only codes with provisions for wind loading incorporating torsion load. Two approaches are used in the codes to assess wind-induced torsional loads on buildings. In the first approach, reduced wind load is applied with some eccentricity from the center of the building. However, in the second approach, non-uniform load is applied by introducing

partial loading on part of the face or triangular loading. In this paper Indian standard [31] is used for estimating the wind force coming on the structure. ASCE 7-22 recommended the directional method for main wind force resisting systems (MWFRS) of building. Table 1 shows the wind load cases that must be considered when designing MWFRS for buildings of all heights. P_{WX} and P_{LX} are considered equal here and it is equal to p_d as detailed in Table 2.

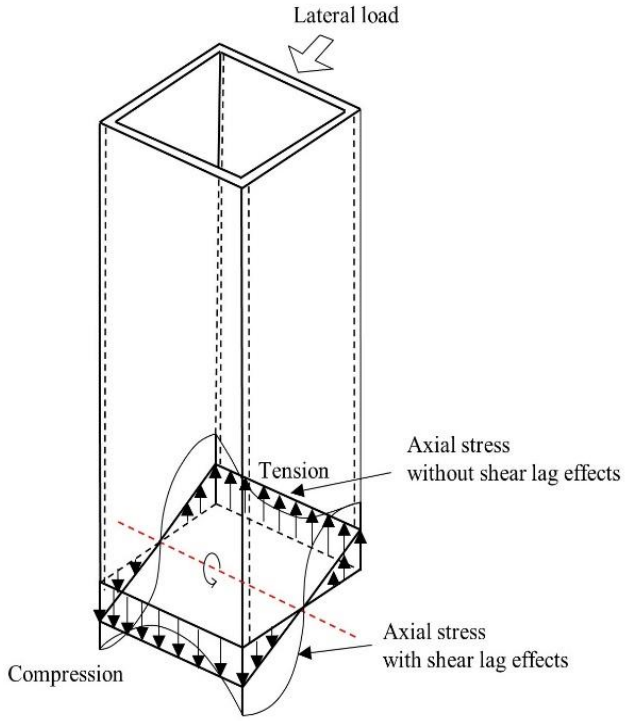

Fig. 2. Framed tube building with and without shear lag effects.

2.1. ASCE 7-22: 2022

For estimating wind loads on MWFRS, ASCE/SEI 7-22 provides two analytical methods: (i) the simplified (envelope) method is applicable to buildings under 18.288 meter in height, and (ii) the detailed (directional) method applies to buildings of any height. ASCE 7-22 recommended the directional method for MWFRS of tall building. Fig. 3 shows the wind load cases that must be considered when designing MWFRS for buildings of all heights. M_T in case 2 is calculated as

$$MT = 0.75\ (PWX + PLX)\ BX\ eX \quad (1)$$

and in case 4,

$$MT = [0.563\ (PWX + PLX)\ BX\ eX + 0.563\ (PWZ + PLZ)\ BZeZ \quad (2)$$

Where, $e_x = \pm\ 0.15B_X$ and $e_z = \pm\ 0.15B_Z$. and the building plan dimensions considered are B_X = 30 m, and B_Z = 35 m.

2.2. NBCC 2020

There are two analytical procedures provided in NBCC 2020 for predicting wind loads on buildings. The first is a static method used for low rise (H < 20m) and medium rise (H = 20-60m) buildings while the second method, namely, dynamic method, is used for high rise buildings (H > 60m). However, for medium rise and high-rise buildings four load cases are specified in Fig. 3 (full and partial wind loads). In Cases A and C, structure is subjected to uniform wind load for calculating maximum base shear while in Cases B and D, structure is subjected to partial loading to produce torsion.

3. Modelling and analysis

3.1. Building dimensions

A model of 40 storey RCC framed tube building is analyzed using STAAD-pro software. Specification of the building taken from Singh *et al*. [32], the height of the building is 120 meters and each floor has a height of 3 meters; the plan dimensions of the framed tube are 35 meters along X-axis and 30 meters along Z-axis (Fig. 4); the beam and column sizes are 0.8m × 0.8 m; the center-to-center spacing of the columns is 2.5 meters in each direction, and the modulus of elasticity (E) is 20 GPa and Poisson's ratio (ν) is 0.15. Also, a uniform dead load of 3.43 kN/m^2 has been considered for all the cases.

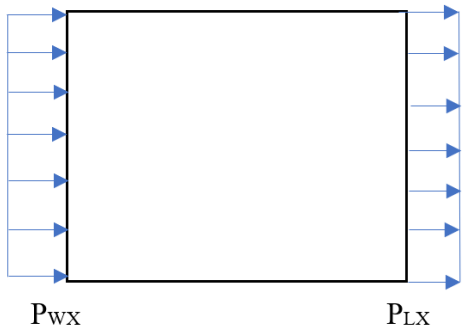

ASCE CASE 1/ NBCC CASE-A

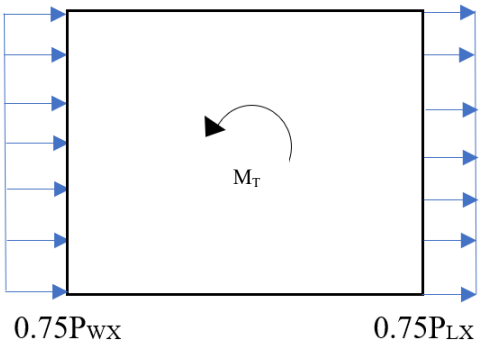

ASCE CASE-2

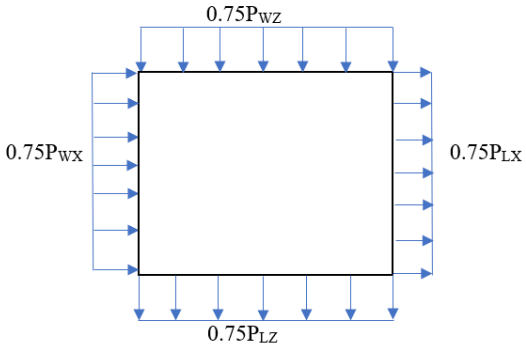

ASCE CASE-3/ NBCC CASE-C

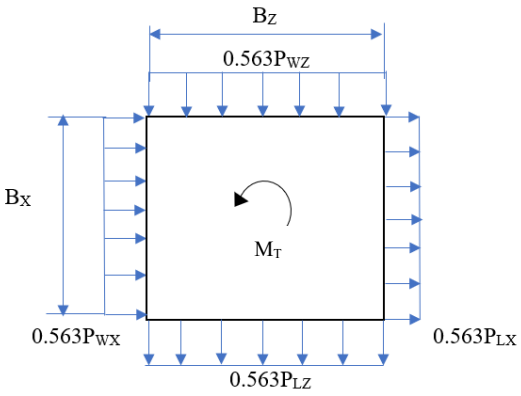

ASCE CASE-4

NBCC CASE-B

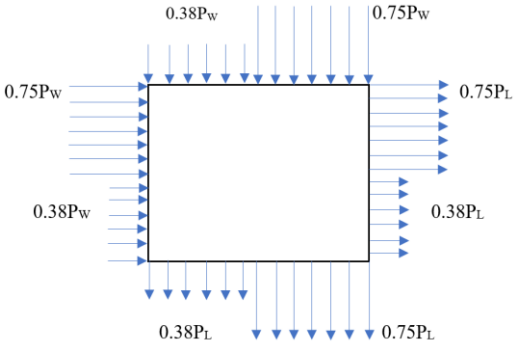

NBCC CASE-D

Fig. 3. Six different wind load Cases taken from ASCE 7-22 and NBCC 2020.

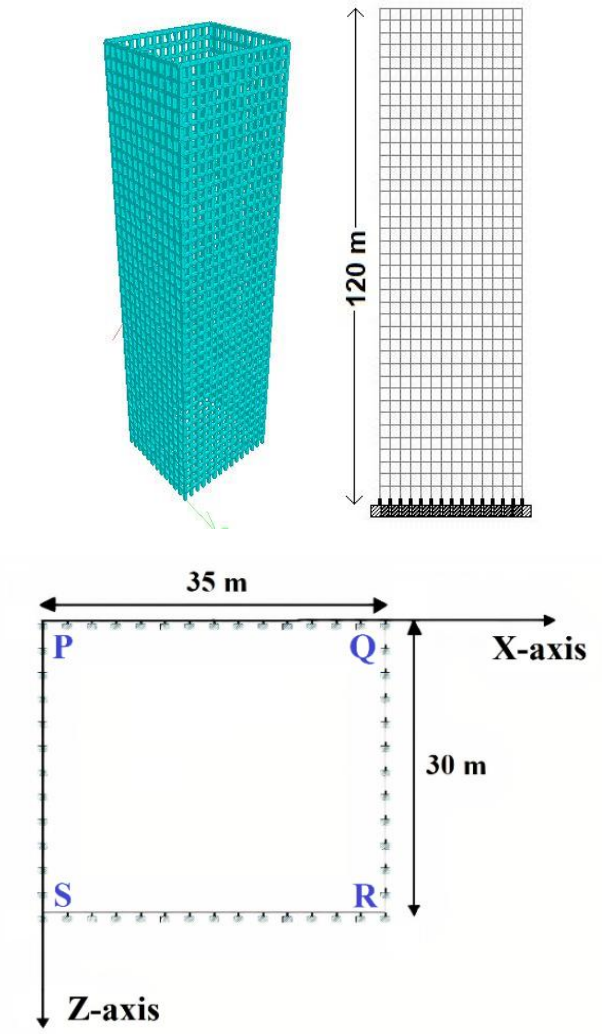

Fig.4. Plan,Elevation and Isometric view of STAAD-pro building model.

3.2. Calculation of wind pressures

Wind pressure calculations have been done as per clause 6.3 (Design Wind Speed) and clause 7.2 (Design Wind Pressure) of code IS 875 (Part 3): 2015 [31]. All the parameters used in calculating wind load and their respective values are listed in Table 1. Design wind speed (V_z) is calculated for terrain category 1 using Equation 3. Velocity (V_z) is varying with height as coefficient k_2 changes with height.

$$Vz = Vb.k1.k2.k3.k4 \quad (3)$$

Description and values of all the parameters are given in Table 1 except the k_2 which is terrain roughness and height factor, values of k_2 are given in Table 2. Design wind pressure is calculated using Equation 4.

$$pd = pz.Ka.Kc.Kd \quad (4)$$

Where, $p_z = 0.6.\ (V_z)^2$, K_a, K_c and K_d is are given in Table 2.

Table 1. Specification of the wind load.

Parameters and Descriptions	Values
Basic wind speed (Vb)	55(m/s)
Terrain Category	1
Probability factor (k1)	1.08
Topography factor (k3)	1
Importance factor for cyclonic region (k4)	1
Area averaging factor (Ka)	0.8
Wind directionality factor (Kd)	0.9
Combination factor (Kc)	0.9

3.3. Wind load cases applied on the building

Each of the codes, ASCE 7-22 and NBCC 2020, recommends four cases. However, two of the loading cases are exactly the same in both the codes, thus making for a total of six cases. Therefore, in this paper, a total of six load cases are analyzed based on the recommendations of the ASCE 7-22 and NBCC 2020 codes, which encompass most of the load cases.

Table 2. Wind velocity and pressure with height.

Height (m)	V_b (m/s)	k_1	k_2	k_3	k_4	V_z (m/s)	p_z (N/m^2)	p_d (kN/m^2)	0.75p_d (kN/m^2)	0.563p_d (kN/m^2)	0.38p_d (kN/m^2)
10	55	1.08	1.05	1	1	62.37	2334.01	1.51	1.13	0.85	0.57
20	55	1.08	1.12	1	1	66.53	2655.58	1.72	1.29	0.97	0.65
30	55	1.08	1.15	1	1	68.31	2799.75	1.81	1.36	1.02	0.69
40	55	1.08	1.18	1	1	69.80	2922.81	1.89	1.42	1.07	0.72
50	55	1.08	1.20	1	1	71.28	3048.50	1.98	1.48	1.11	0.75
60	55	1.08	1.21	1	1	71.99	3109.78	2.02	1.51	1.13	0.77
70	55	1.08	1.22	1	1	72.71	3171.66	2.06	1.54	1.16	0.78
80	55	1.08	1.24	1	1	73.42	3234.16	2.10	1.57	1.18	0.80
90	55	1.08	1.25	1	1	74.13	3297.26	2.14	1.60	1.20	0.81
100	55	1.08	1.26	1	1	74.84	3360.97	2.18	1.63	1.23	0.83
110	55	1.08	1.27	1	1	75.32	3403.79	2.21	1.65	1.24	0.84
120	55	1.08	1.28	1	1	75.79	3446.87	2.23	1.68	1.26	0.85

4. Results and discussion

This section discusses the results obtained from the analyses based on the six load cases. Variations in shear lag are studied due to six different loading cases on a 40-storeyed tubular building. Axial force in columns of short edge (QR- face) and long edge (SR-face) is plotted for 1st storey, 10th, 20th, 30th and 40th storey in Fig. 5 -10. Moreover, the comparison has been done between different load cases separately for single direction loadings (ASCE Case-1 or NBCC Case-A, ASCE Case-2 and NBCC Case-B loadings) and two direction loadings (ASCE Case-3 or NBCC Case-C, ASCE Case-4 and NBCC Case-D loadings). Throughout the discussion, it is to be noted that the short edge panel refers to QR - face and the long edge panel refers to SR- face (Fig. 4).

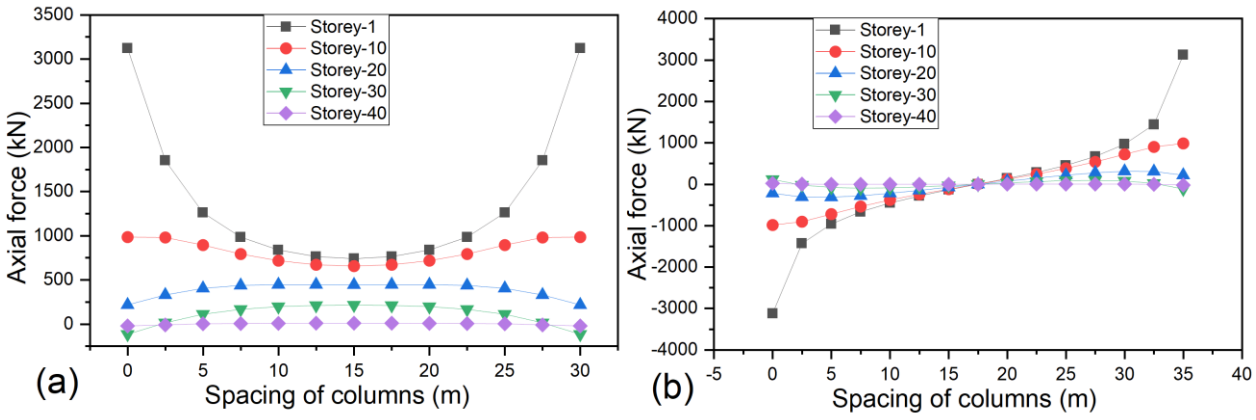

Fig. 5. Axial force in **(a)** short edge and **(b)** long edge panel's columns for ASCE Case-1/NBCC Case-A loading.

4.1. Shear lag due to ASCE case-1/NBCC case-a loading

In Fig. 5, axial force distribution in short edge and long edge panel columns at the ground storey and stories 10^{th}, 20^{th}, 30^{th} and, 40^{th} for ASCE Case-1/NBCC Case-A loading are shown. From Fig. 5(a), it is observed that axial force in 1st storey of short edge panel is maximum in corner column. The axial force decreases as one moves toward the center of the short edge panel and it becomes minimum at middle column. This distribution is called as positive shear lag, *i.e.*, corner columns have more axial force than middle columns. As storey height increases, axial force in corner column decreases when compared to central column. At storeys nearly 11^{th} to 13^{th} axial force in column adjacent to corner column becomes maximum. This trend continues as height increases and ultimately leads to the occurrence of negative shear lag at the 20^{th} storey. At 30^{th} storey, axial force in corner columns is tensile in nature. With a further increase in height, axial force in corner columns increases and continues to be tensile. At storeys near to the top of the building, the axial force decreases but remains in tension which needs to be considered by the designer appropriately. In Fig. 5(b), axial force distribution for the long panel, axial force in corner column S is tensile and column R is compressive. As height increases, axial force in the corner column decreases as compared to adjacent columns. From storeys near to 30^{th} storey, axial force in corner column again increases but in opposite nature. At 40^{th} storey, axial force again decreases to some extent but remains in the same pattern as 30^{th} storey.

4.2. Shear lag due to ASCE case-2 loading (including torsion)

In Case of ASCE Case-2 loading (which includes torsional moment), axial force distribution in short edge and long edge columns at the 1st storey and 10, 20, 30 and 40 storeys are shown in Figs. 6(a) and 6(b). From the figures, it can be seen that the distribution of axial force along both the panel is similar to that ASCE Case-1 which have no torsion. However, in this case, the magnitude of axial force gets reduced due to the application of partial (75% of ASCE case -1) loading. Axial force in columns on either side of middle column has a small difference in magnitude, *i.e.*, not symmetrical about central column as in the ASCE Case-1 loading. At base storey, axial force in corner columns and central column is reduced by 24% and 24.9% respectively than that of corresponding columns in ASCE Case-1, which conforms to the reduction of 25% in the load values. Here, also negative shear lag occurs near around below 20^{th} storey as in previous case but after that with the increase in height axial force in corner columns again increases in opposite direction. At top storey axial force in corner columns and middle column get reduced by 24.64% and 24.9% respectively than that of ASCE Case-1. In long edge panel, axial force in columns is less than that evaluated in non-torsional loading Case (*i.e.*, Case-1). Axial force in corner columns of 1st storey is approximately 25.64% lesser than corresponding column of previous case whereas in middle column axial force get reduced by 25%.

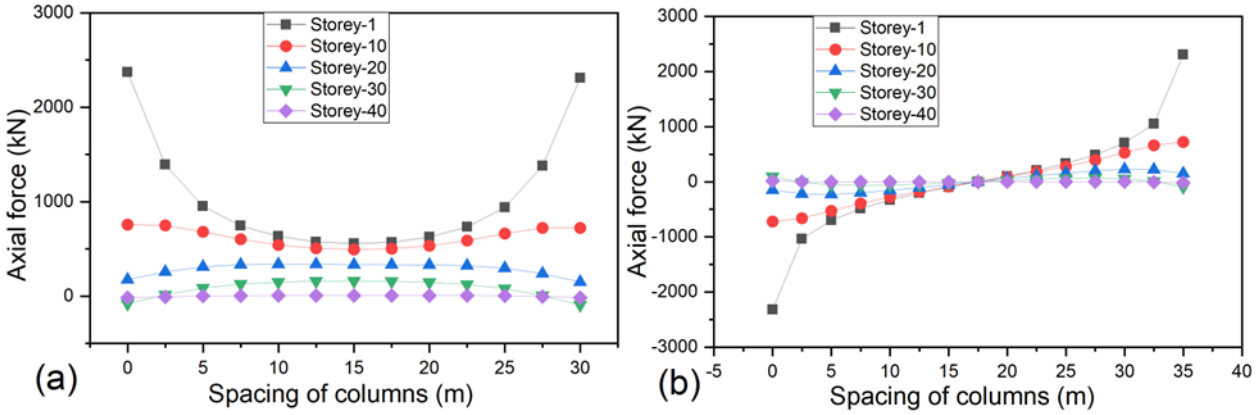

Fig. 6. Axial force in **(a)** short edge and **(b)** long edge panel's columns for ASCE Case-2 loading.

4.3. Shear lag due to NBCC case-B loading

Axial force distribution due to NBCC Case-B loading in short edge and long edge panel columns are shown in Fig. 7(a) and 7(b). It can be seen from Fig. 7 that the distribution of axial force is significantly different from ASCE Case-1/NBCC Case-A (refer Fig. 5). The distribution of axial force (Fig. 7 a) in short edge panels is not symmetrical around the central column. Since the loading is acting on half of the building, close to corners Q, the axial force is greater in column Q. Positive shear lag is observed in some storeys near the base and the 10th storey. From the 20th storey, negative shear lag occurs where the corner columns on both sides have less axial force than the central column. As height increases, the axial force in the corner column changes its nature and increases in the opposite direction. Near the 30th floor, axial forces on corner columns become tensile and near the top stories, they decrease again but remain in tension. Whereas in long edge panel the axial force distribution is similar to ASCE Case-1 loading but smaller than in ASCE Case-1 and 2 loading. Axial force in the corner column is maximum at the base which is 72.9% lesser than axial force in the corresponding column in ASCE Case-1/NBCC Case-A loading. Axial force in the central column is approximately near zero for top storeys. Similar to previous cases, the axial force in corner columns decreases as the height increases.

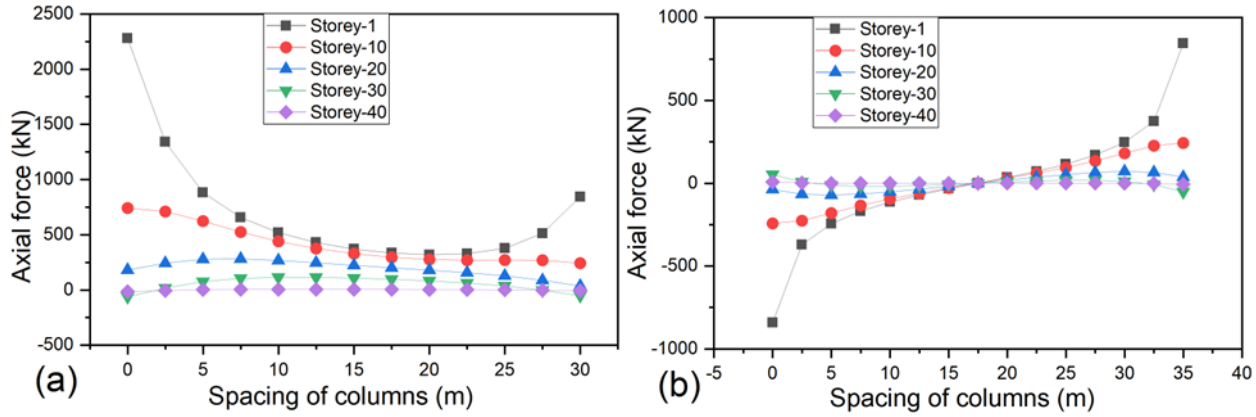

Fig.7. Axial force in **(a)** short edge and **(b)** long edge panel's columns for NBCC Case-B loading.

4.4. Shear lag due to ASCE case-3/NBCC case-c loading

This section discusses the results obtained for the loading ASCE case 3/ NBCC Case - C, as shown in Fig. 8. The results obtained from this loading pattern become more prominent than the normally adopted loading pattern (ASCE Case-1/ NBCC case-A). This case gives the axial force of 5510 kN in column R compared to 3120 kN in case 1. This increase is approximately 1.77 times that of loading case 1. As shown in Fig 8(a) and 8(b), axial force distribution is similar in short edge and long edge. In this case, the axial force in column Q is much lesser than in column R. The long edge corner column S has much lesser axial force than corner column R.

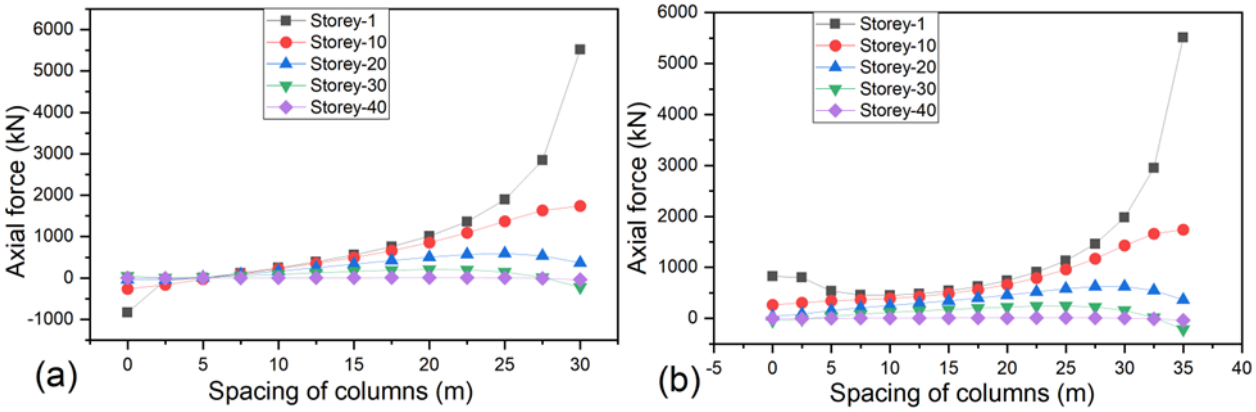

Fig. 8. Axial force in **(a)** short edge and **(b)** long edge panel's columns for ASCE Case-3/NBCC Case-C loading.

4.5. Shear lag due to ASCE case-4 loading

Axial force distribution shown in Figs. 9(a) and 9(b) are similar to that in case of ASCE Case-3 loading but the magnitude of force is reduced due to applied partial (56.3% of P_W) loading. Similar to the ASCE Case-3 loading, shown in Fig. 9(a), the axial force in corner column Q is negative and is positive in corner column R which has a higher magnitude than corner column Q at 1st storey. As height increases, axial force in corner columns decreases and nearly at the 20th storey, axial force in columns adjacent to corner column is larger than corner column. At stories near to 30th storey axial force in the corner column again increases but in the opposite direction and it again decreases towards the top stories but remains in tension. However, in long edge panel axial force distribution is not symmetrical about the middle column because loads are acting on both the faces. Axial force in corner column R of 1st storey is quite higher than other columns of the same level. From Fig. 9(b), it can be observed that storeys near to base shows positive shear lag similar to Fig.8 (b) of ASCE Case-3 loading. As height increases axial force in corner columns decreases and from storeys near to 20th storey negative shear lag is occurred. With further increase in height, axial force in corner column increases in tensile nature.

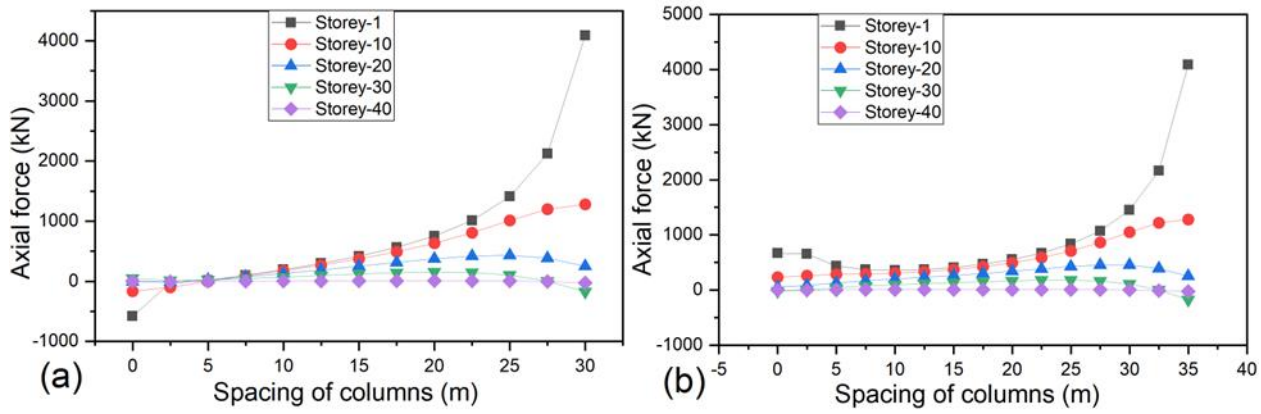

Fig. 9. Axial force in **(a)** short edge and **(b)** long edge panel's columns for ASCE Case-4 loading.

The results from this case are similar to the ASCE case 3 loading but with the lesser magnitude because the axial loading is 25% lesser in this case. At corners, the axial force is 26% lesser than the ASCE case 3 loading, this difference is due to additional torsional moment M_T.

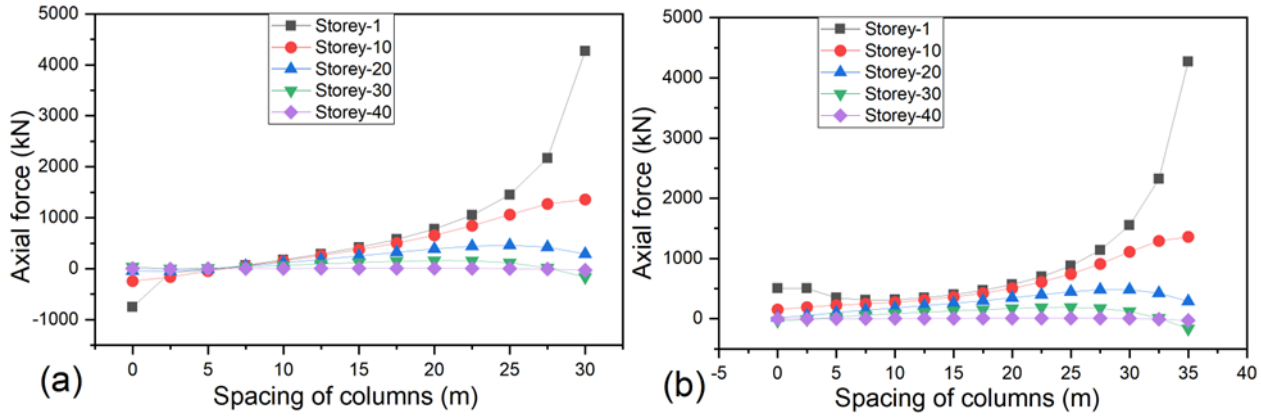

Fig. 10. Axial force in **(a)** short edge and **(b)** long edge panel's columns for NBCC Case-D loading.

4.6. Shear lag due to NBCC case-d loading

Figs.10 (a) and 10 (b) demonstrate shear lag in tubular buildings due to NBCC Case-D loading. The Axial force distribution along both panels is similar to that of ASCE Case-3/NBCC Case-C and ASCE Case-4 loadings, and the magnitude of the axial force is in between both types of loadings. In this case, due to varying partial loadings (ref. Fig. 3), which cause torsion in the building, the axial force in columns is lesser than ASCE Case-3/NBCC Case-C loading. However, it is more than ASCE Case-4 loading. Axial force is very high in corner column R at the base as compared to other columns of the same storey due to torsion. In corner columns, axial force decreases with height, and in adjacent columns, it increases as compared to corner columns up to a certain storey. With further increase in height, axial force in corner columns changes its behavior, becomes tensile in nature. Axial force in corner column R of base storey is higher than other columns of base storey. From Fig. 10 (b), it can be seen that storeys near to base shows positive shear lag similar to Fig. 8(b) of ASCE Case-3/NBCC Case-C loading.

5. Comparison of axial forces due to different loading cases

5.1. Axial force due to loading in one direction

This section compares the results obtained from ASCE Case-1/NBCC Case-A, ASCE Case-2, and NBCC Case-B loadings on a tubular tall building. Due to their single-direction loading, these three loading patterns are chosen for comparison. Axial forces in columns are compared at the level of 1st, 20th, and 40th storey. Fig. 11 describes the variation of axial forces in columns for these three different levels of the buildings corresponding single direction loading. As expected, the top storey columns experience the tensile nature of axial forces. It can be noted that for loading NBCC case-B, the pattern of axial force distribution is different from the other two loading cases, because of the partial loading.

5.2. Axial force due to loading in two direction

This section compares the shear lag effects obtained from loading as per ASCE Case-3/NBCC Case-C, ASCE Case-4, and NBCC Case-D loadings on a tubular tall building. It was chosen to compare these three loading patterns because load is acting in both directions. The 1st storey, 20th storey, and 40th storey are taken into account when comparing axial forces in column. Fig. 12 depicts the variation of axial forces for the three different levels of the buildings corresponding to two direction loading. The top storey columns experience the tensile nature of axial forces. Here, it is important to emphasize that the variation of axial forces is unsymmetrical about the central axes of the building. Also, it is interesting to note that the magnitude of axial force in corner Q is negative at the first storey itself. This is due to the multi-directional wind loading pattern. None of the previous studies on shear lag effect of tall tubular building subjected to lateral load reported this uncertainty. While designing such buildings, these recommended loading patterns should be carefully considered.

6. Axial forces in the corner columns

The following table further highlights the importance of the present study in the context of shear lag effect. So far, existing studies used to consider lateral loading in single face only [32]. However, in the present study, all load cases are providing wind load on the building on two or more faces. Interestingly, ASCE Case -3/NBCC case-C give an axial load in corner columns P and R having magnitudes 1.76 times that of ASCE Case -1/NBCC case-A. Similarly, ASCE Case-4 and NBCC Case-D gives higher results as can be seen from the Table 3.

Table 3. Axial forces in the 1st storey of corner columns for all the loading case.

Loading Cases	Axial force in Column P (kN)	Axial force in Column Q (kN)	Axial force in Column R (kN)	Axial force in Column S (kN)
ASCE Case - 1/NBCC case-A	-3120	3120.00	3120.00	-3120.00
ASCE Case -2	-2370	2370.00	2310.00	-2320.00
ASCE Case - 3/NBCC case-C	-5520	-833.14	5510.00	827.09
ASCE Case -4	-4190	-578.68	4090.00	667.60
NBCC case-B	-2280	2280.00	843.09	-842.66
NBCC case-D	-4040	-749.20	4270.00	503.33

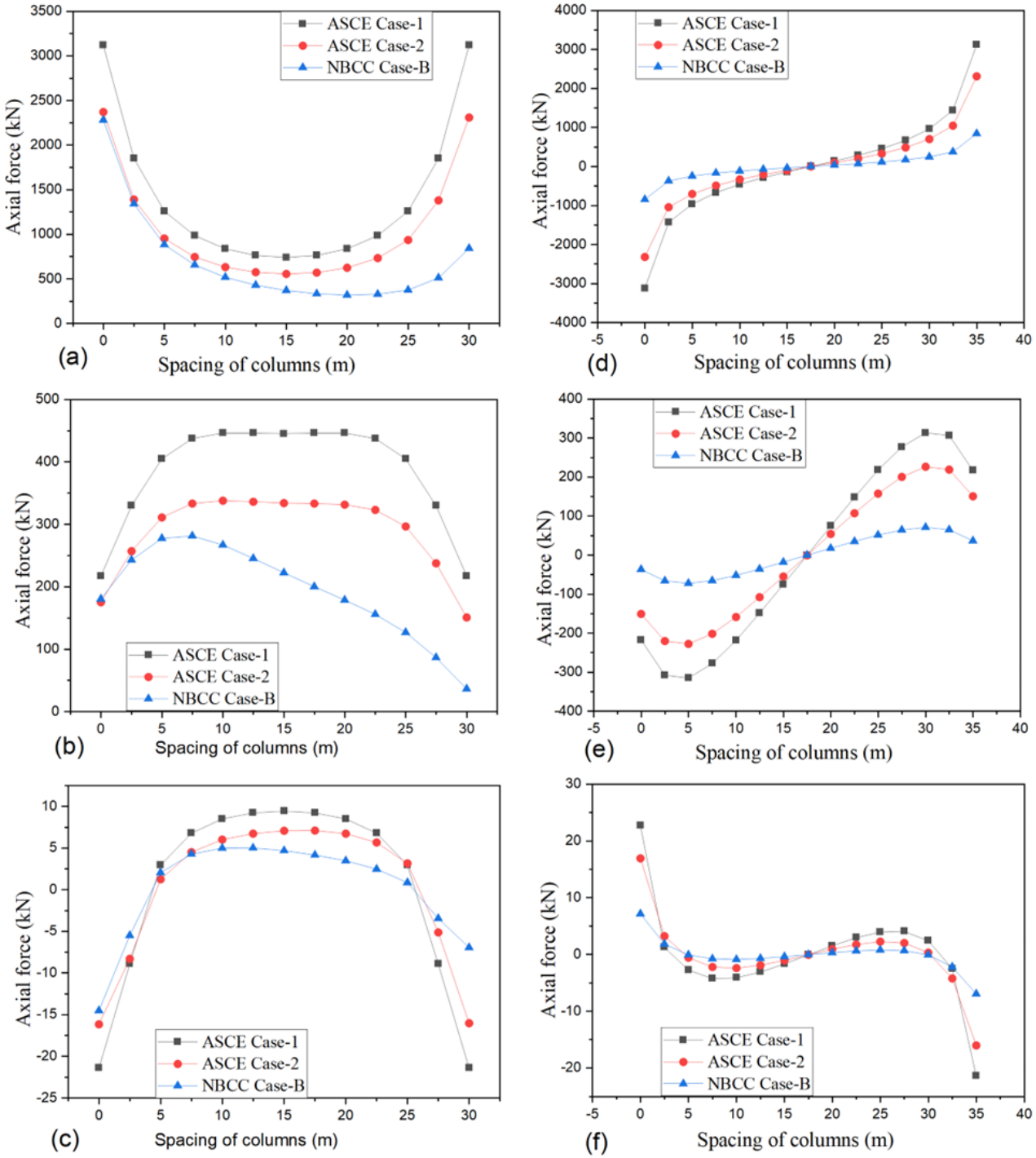

Fig. 11. Comparison of axial forces of single direction loading cases (ASCE Case-1, ASCE Case-2 and NBCC Case-B), Axial force in short edge panel's columns of 1st **(a)**, 20th **(b)**, and 40th **(c)** storey; Axial force in long edge panel's columns of 1st **(d)**, 20th**(e)**, and 40th **(f)** storey.

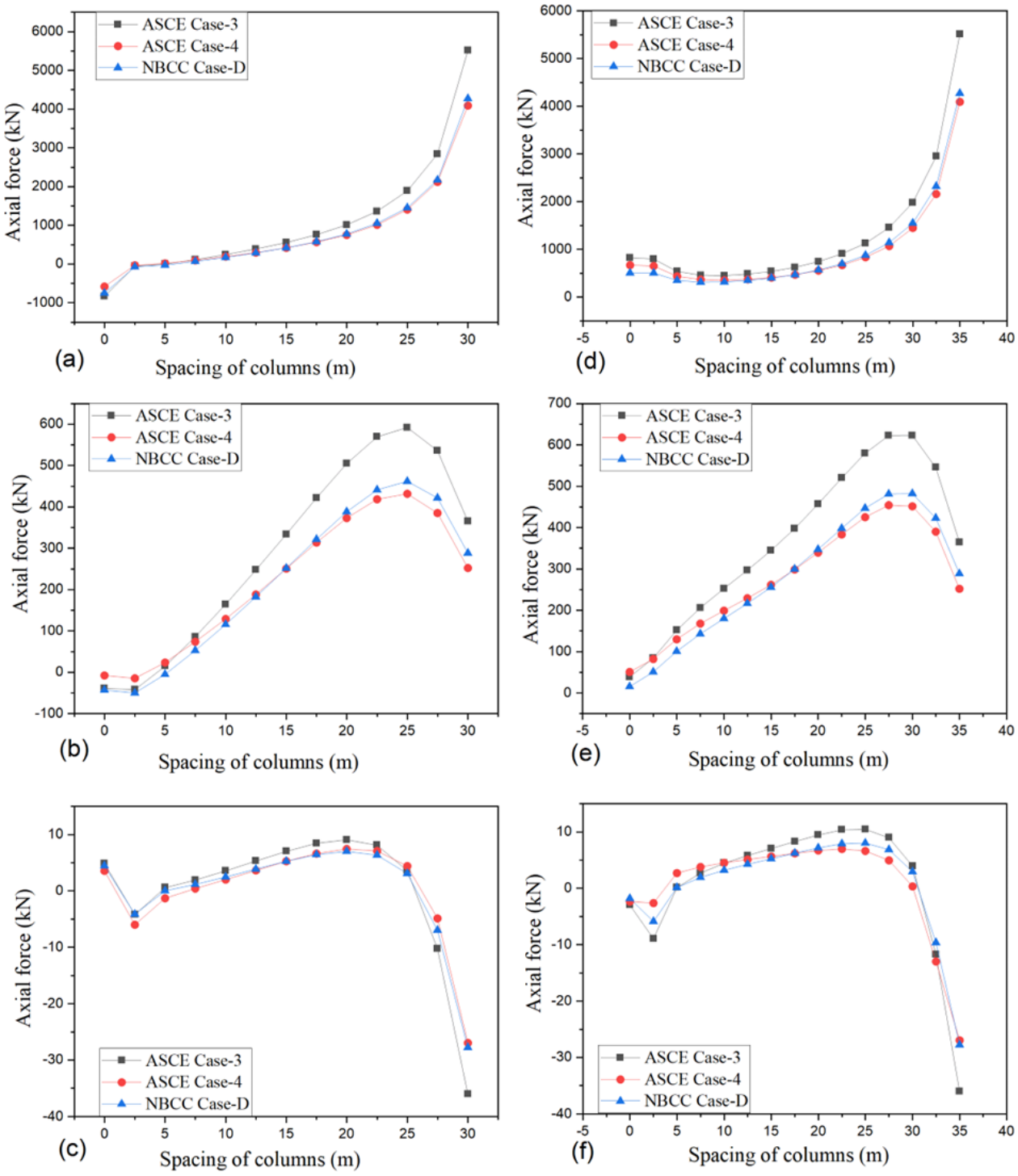

Fig. 12 Comparison of axial forces of two direction loading cases (ASCE Case-3, ASCE Case-4 and NBCC Case-D), Axial force in short edge panel's columns of 1st **(a)**, 20th **(b)**, and 40th **(c)** storey; Axial force in long edge panel's columns of 1st **(d)**, 20th **(e)**, and 40th **(f)** storey.

7. Conclusion

This study investigates the variation in the shear lag phenomenon for a 40-storey RCC framed tube building using STAAD-pro software. Six different wind load patterns given in ASCE 7-22 and NBCC-2020 codes for the tall building have been considered. These patterns include uniform loading on all faces as well as non-uniform loading combined torsional moments. Also, two

loading cases consist of partial loading applied to the faces of the building. The change in the shear lag phenomenon of the building is critically discussed in section 4 and comparisons are drawn in Section 5. The results from this study help in understanding the effect of various wind loading patterns on the shear lag phenomenon of tubular tall structures. Based on the results, the following conclusions can be drawn regarding variations in shear lag:

- Axial force distribution also changes with changing load patterns. For NBCC Case-B, where loading is only on half of the face, axial force distribution becomes unsymmetric. In addition, there is a significant difference between axial force distributions of load cases with both directions of loading and those with only one direction of loading.
- ASCE Case -3/NBCC case-C give an axial load in corner columns P and R having magnitudes 1.76 times that of ASCE Case -1/NBCC case-A.
- Comparing the axial force distribution at corner columns, in case of single face loading at 1st storey indicates that axial force in case of uniform one direction loading case (ASCE Case-1/NBCC Case-A) is more than the loading cases including torsional moment (ASCE Case-2 and NBCC Case -B). Axial force in case of NBCC Case -B loading is lower than ASCE Case-1/NBCC Case-A and ASCE Case-2 loadings. While in the case of ASCE Case-2 loading, it is in between these two loadings.
- In the case of both face loadings, comparison of the axial force distribution at 1st storey indicates that axial force in the uniform loading case (ASCE Case-3/NBCC Case-C) is also more than the loading cases including torsional moment (ASCE Case-4 and NBCC Case-D). But the difference in axial force distribution in the case of ASCE Case-4 and NBCC Case-D loadings is insignificant.
- The results from ASCE Case-4 and NBCC Case-D are close to each other both in magnitude as well as in their nature of variation.

Conflict of interest

On behalf of all authors, the corresponding author states that there is no conflict of interest.

References

[1] Kuzmanović BO, Graham HJ. Shear Lag in Box Girders. J Struct Div 1981;107:1701–12. https://doi.org/10.1061/JSDEAG.0005777.

[2] Lee SC, Yoo CH, Yoon DY. Analysis of Shear Lag Anomaly in Box Girders. J Struct Eng 2002;128:1379–86. https://doi.org/10.1061/(ASCE)0733-9445(2002)128:11(1379).

[3] Rovňák M, Ďuricová A. Discussion of "Analysis of Shear Lag Anomaly in Box Girders" by S. C. Lee, C. H. Yoo, and D. Y. Yoon. J Struct Eng 2004;130:1860–1. https://doi.org/10.1061/(ASCE)0733-9445(2004)130:11(1860).

[4] ZHOU S. Shear lag analysis of box girders. Eng Mech 2008;25:204–8.

[5] Foutch DA, Chang PC. A Shear Lag Anomaly. J Struct Div 1982;108:1653–8. https://doi.org/10.1061/JSDEAG.0005995.

[6] Singh GJ, Mandal S, Kumar R, Kumar V. Simplified Analysis of Negative Shear Lag in Laminated Composite Cantilever Beam. J Aerosp Eng 2020;33. https://doi.org/10.1061/(ASCE)AS.1943-5525.0001100.

[7] Singh Y, Nagpal AK. Negative Shear Lag in Framed-Tube Buildings. J Struct Eng 1994;120:3105–21. https://doi.org/10.1061/(ASCE)0733-9445(1994)120:11(3105).

[8] Rovňák M, Rovňáková L. Discussion: Negative Shear Lag in Framed-Tube Buildings. J Struct Eng 1996;122:711–3. https://doi.org/10.1061/(ASCE)0733-9445(1996)122:6(711).

[9] Khan FR, Amin NR. Analysis and design of framed tube structures for tall concrete buildings. Spec Publ 1972;36:39–60.

[10] Coull A, Bose B. Simplified analysis of frame-tube structures. J Struct Div 1975;101:2223–40.

[11] Haji-Kazemi H, Company M. Exact method of analysis of shear lag in framed tube structures. Struct Des Tall Build 2002;11:375–88. https://doi.org/10.1002/tal.208.

[12] Mahjoub R, Rahgozar R, Saffari H. Simple method for analysis of tube frame by consideration of negative shear lag. Aust J Basic Appl Sci 2011;5:309–16.

[13] Leonard J. Investigation of shear lag effect in high-rise buildings with diagrid system 2007.

[14] Kim J, Lee Y. Seismic performance evaluation of diagrid system buildings. Struct Des Tall Spec Build 2012;21:736–49. https://doi.org/10.1002/tal.643.

[15] Zahiri-Hashemi R, Kheyroddin A, Farhadi B. Effective number of mega-bracing, in order to minimize shear lag. Struct Eng Mech 2013;48:173–93. https://doi.org/10.12989/sem.2013.48.2.173.

[16] Mazinani I, Jumaat MZ, Ismail Z, Chao OZ. Comparison of shear lag in structural steel building with framed tube and braced tube. Struct Eng Mech 2014;49:297–309. https://doi.org/10.12989/sem.2014.49.3.297.

[17] Gaur H, Goliya RK. Mitigating shear lag in tall buildings. Int J Adv Struct Eng 2015;7:269–79. https://doi.org/10.1007/s40091-015-0098-1.

[18] Shi Q, Zhang F. Simplified calculation of shear lag effect for high-rise diagrid tube structures. J Build Eng 2019;22:486–95. https://doi.org/10.1016/j.jobe.2019.01.009.

[19] Mashhadiali N, Molaei F, Siavoshi H. Investigation of shear lag effect in tall tube-type buildings. Structures 2021;34:4204–15. https://doi.org/10.1016/j.istruc.2021.10.035.

[20] Hafner I, Vlašić A, Kišiček T, Renić T. Parametric Analysis of the Shear Lag Effect in Tube Structural Systems of Tall Buildings. Appl Sci 2020;11:278. https://doi.org/10.3390/app11010278.

[21] Moghadasi M, Taeepoor S, Rahimian Koloor SS, Petrů M. The Effect of Lateral Load Type on Shear Lag of Concrete Tubular Structures with Different Plan Geometries. Crystals 2020;10:897. https://doi.org/10.3390/cryst10100897.

[22] Hoseini Vaez SR, Naderpour H, Kheyroddin A. The Effect of RC Core on Rehabilitation of Tubular Structures. J Rehabil Civ Eng 2014;2:63–74.

[23] Tabiee M, Abdoos H, Khaloo A. Concurrent effects of the shear-lag and warping torsion on the performance of non-rectangular RC shear walls. Arch Civ Mech Eng 2023;23:138. https://doi.org/10.1007/s43452-023-00663-1.

[24] Li J, Wang T, Li F, You Y, Kong Z. Experimental and numerical study on the shear lag behavior of l-shaped double-steel-plate composite shear wall. Structures 2023;47:1729–42. https://doi.org/10.1016/j.istruc.2022.11.103.

[25] Kumari S, Singh A, Mandal S. Effect of Terrain Category, Aspect Ratio and Number of Storeys on the Shear Lag Phenomenon in RCC Framed Tube Structures, 2022, p. 163–76. https://doi.org/10.1007/978-3-031-04793-0_12.

[26] Isyumov N, Poole M. Wind induced torque on square and rectangular building shapes. J Wind Eng Ind Aerodyn 1983;13:183–96. https://doi.org/10.1016/0167-6105(83)90140-X.

[27] Tallin A, Ellingwood B. Serviceability Limit States: Wind Induced Vibrations. J Struct Eng 1984;110:2424–37. https://doi.org/10.1061/(ASCE)0733-9445(1984)110:10(2424).

[28] Minimum Design Loads and Associated Criteria for Buildings and Other Structures.

Reston, VA: American Society of Civil Engineers; 2021. https://doi.org/10.1061/9780784415788.

[29] Commission C, Codes F. National Building Code of Canada Volume 1. vol. 1. 2020.

[30] Tc CEN. Eurocode 1 : Actions on structures — General actions — Part 1-4 : Wind actions Contents. Communities 2004;4:1–148.

[31] Standards B of I. Code of Practice for Design Loads (Other Than Earthquake) for Buildings and Structures - Part 3: Wind Loads 2015.

[32] Singh GJ, Mandal S, Kumar R. Investigation on Shear Lag Phenomenon in RCC Framed Tube Structures. I-Manager's J Struct Eng 2015;4:18–25. https://doi.org/10.26634/jste.4.3.3727.